Evolution of the Silvretta eclogites : metamorphic and magmatic events

Autor(en): **Maggetti, M. / Galetti, G.**

Objekttyp: **Article**

Zeitschrift: **Schweizerische mineralogische und petrographische Mitteilungen = Bulletin suisse de minéralogie et pétrographie**

Band (Jahr): **68 (1988)**

Heft 3: **Geodynamik des eurpäoschen Variszikums : Kaledonisch-Variszische Strukturen in den Alpen**

PDF erstellt am: **11.07.2024**

Persistenter Link: https://doi.org/10.5169/seals-52082

SCHWEIZ. MINERAL. PETROGR. MITT. 68, 467-484, 1988

Evolution of the Silvretta eclogites: metamorphic and magmatic events

by *M. Maggetti*[1] and *G. Galetti*[1]

Abstract

Textural, mineralogical and chemical arguments are used to trace the complex history of the Silvretta eclogites which can be divided into one igneous and five metamorphic episodes: I) Formation of basaltic/gabbroic precursor rocks by crystallization from tholeiitic MORB-like liquids at spreading ridges after continental breakup or in marginal basins. The geochemical characteristics are consistent with strong differentiation due to olivine + plagioclase + clinopyroxene + spinel fractional crystallization at shallow depths. II) First penetrative deformation under lower amphibolite facies conditions. III) HP event with two deformations. Chemical zoning of garnets and inclusions in garnets and omphacites indicate a multistage prograde recrystallization. Conditions of at least 14–16 kb and 550–650 °C for the metamorphic peak are deduced from chemical analyses of garnet/omphacite contact pairs in equilibrium eclogites. H_2O-fluids caused growth of Ca-amphiboles and zoisites after the metamorphic peak. Whole-rock chemistry is affected for some elements by these metamorphic overprints. IV) Isothermal (?) pressure release is recorded in symplectitic replacement of omphacite (12–13 kb for assumed 550–650 °C). V) During Variscan times, a penetrative deformation of higher amphibolite facies grade (5.5–7.5 kb/600–650 °C, FLISCH 1987) lead to the formation of garnet-amphibolites resp. plagioclase-amphibolites. VI) Last metamorphic overprint under eo-Alpine (FLISCH, 1986) greenschist-anchizonal facies conditions.

Keywords: Eclogite, magmatic differentiation, metamorphic evolution, mineral chemistry, geochemistry, Silvretta, Swiss Alps.

1. Introduction

The Austroalpine Silvretta nappe covers about 750 km² in Switzerland. In this area, unaltered eclogites (THIERRIN, 1982, 1983; MAGGETTI and GALETTI, 1984; MICHAEL, 1985; MAGGETTI et al., 1987) as well as altered eclogites, i.e. symplectitic garnet amphibolites (SPITZ and DYHRENFURTH, 1914; STRECKEISEN, 1928; SPAENHAUER, 1932; FRAPOLLI, 1975) occur. Similar outcrops were reported by HOERNES (1971) and THÖNI (1988) from the Austrian part of the Silvretta.

Fig. 1 shows the distribution of both eclogitic rock types. The retrograded varieties cover the whole area whereas the unaltered eclogites are confined to the southeastern parts of the Silvretta. This spatial arrangement and the apparently sharp boundary between unaltered and altered eclogites (which cuts across the major tectonic structures, the so-called Schlingen) suggests that the HP event leading to the formation of eclogites has affected the ancient basic and neighbouring sedimentary rocks throughout the whole area and that the retrograde overprint was later than the "Schlingen"-deformation.

The eclogitic rocks of the Silvretta occur as small subconcordant bodies in amphibolites or medium grade paragneisses. Most outcrops show a marked layering which is due to changing grain-size and/or varying amounts of

[1] Institut für Mineralogie und Petrographie der Universität Freiburg i. Ue., Pérolles, CH-1700 Freiburg.

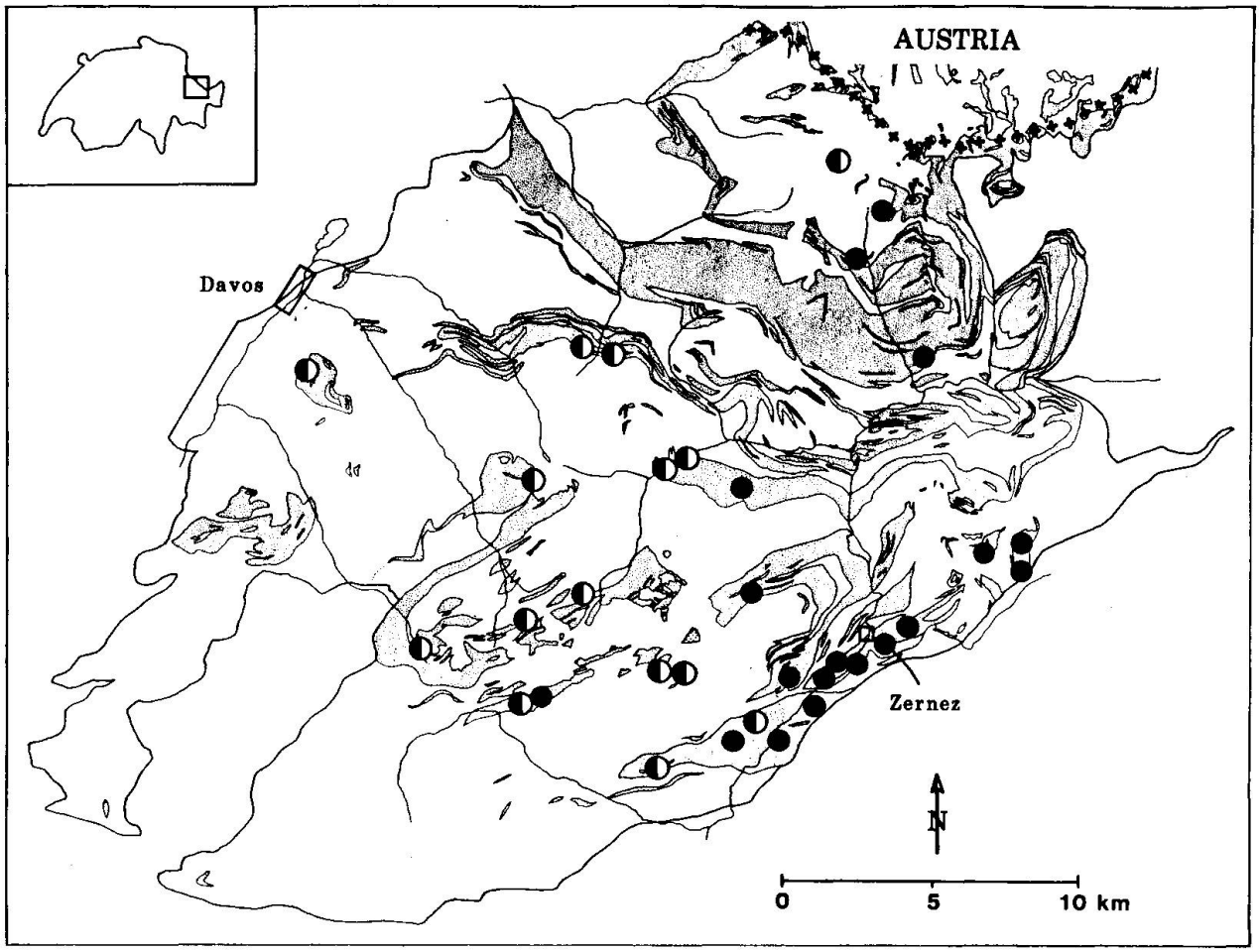

Fig. 1 Distribution of unaltered eclogites (dots) and altered eclogites (half-filled circles) in the Swiss part of the Silvretta. Dotted areas are metabasic terrains after STRECKEISEN (1928), BEARTH (1932a, b), SPAENHAUER (1932) and WENK (1934).

garnet, omphacite or zoisite. The boundaries between singular layers are sharp. Completely unaltered eclogites are not very common. Usually they form small pods in the retrograded varieties. The layers have been isoclinally folded and foliated. Omphacite, amphibole and zoisite are aligned parallel to the layering. Based on microscopic arguments, this deformation must have occured during the high pressure metamorphism. The folds, the layering and the foliation planes have the same orientation as those of the surrounding medium-grade country rocks (phase D2 of FLISCH, 1987).

2. Metamorphic petrology

In 1982 and 1983 THIERRIN first published an evolution model for the Silvretta eclogites. Based on the pre-eclogitic mineral assemblage of plagioclase + amphibole + quartz ± ilmenite ± Ti-augite, he proposed three eclogite and five post-eclogite phases of crystallization combined with three phases of deformation. He estimated for pressures of 12–25 kb temperatures between 698 and 730 °C for the high-pressure event. KRÄHENBÜHL (1984) postulated values of 7 kb and 680 °C, based upon pyroxene-relicts in symplectitic garnet amphibolites. MAGGETTI and GALETTI (1984) published on the basis of microprobe analyses of 21 garnet/omphacite pairs PT conditions of minimum 15–22 kb and 650–750 °C. MICHAEL (1985, 1986) deduced conditions of 9–12 kb and 530–650 °C. Since 1982, more eclogite sites have been discovered in the Silvretta and the results of the detailed petrographic studies are only partially consistent with the conclusions published so far.

2.1. EVOLUTION HISTORY

The eclogites are structurally divided into two types:

eclogite A: fine grained, garnet rich, strongly foliated
eclogite B: medium grained, more or less foliated layers

The following mineral phases are characteristic of eclogites with little retrograde overprint: garnet, omphacite, quartz, Ca-amphibole, zoisite, clinozoisite, white mica, biotite, ilmenite, pyrite, rutile, plagioclase, apatite, zircon and sphene. In eclogites of type A chemically homogeneous and inclusion-poor garnet and omphacite as well as quartz and rutile predominate. Textures indicate equilibrium conditions. In contrast, B-type eclogites which prevail in the field, are characterized by textures and mineral assemblages which reflect the succession of several crystallization and deformation phases. The following outline of the evolution of the Silvretta eclogites is based on the microscopic investigation of B-type eclogites (Fig. 2):

Stage 1: This pre-eclogite event is represented by small inclusions (< 0,3 mm) in the central parts of garnet cores. While inclusions occur randomly in other minerals, abundant inclusions of sphene I, quartz, clinozoisite I, Ca-amphibole I, ilmenite, pyrite, white mica and biotite are concentrated in the cores (max. 8 mm ∅) of large rounded garnet. In a few samples, tiny plagioclase I (An-content: ?) is observed. The grains of clinozoisite I, plagioclase I, quartz and Ca-amphibole I are corroded. These inclusions are orientated and reflect an old s_1 that has been overgrown and preserved by the garnet I. This internal fabric crosscuts the main schistosity s_3 (Fig. 3a). A further proof of the syntectonic nature of the garnet cores (garnet I) is the sigmoidal orientation of in-

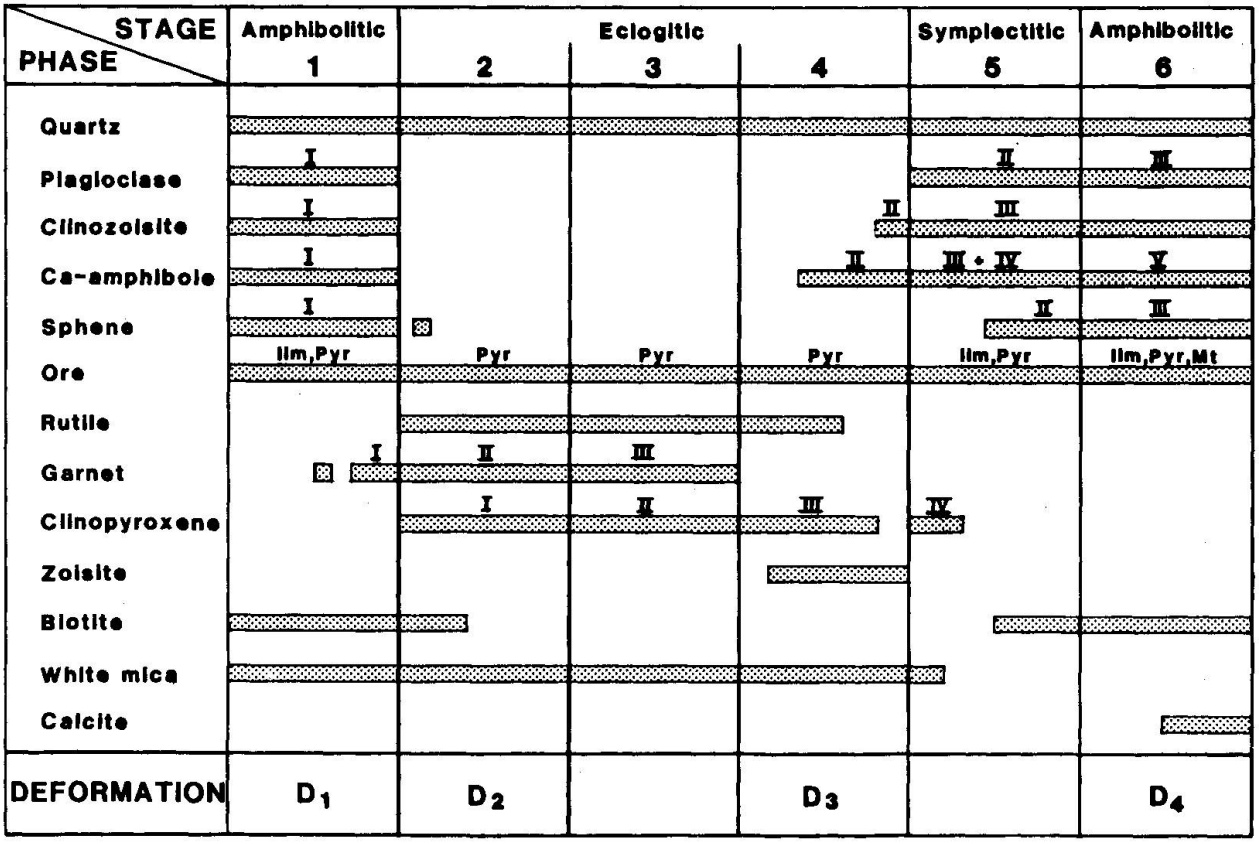

Fig. 2 Scheme of the metamorphic evolution of Silvretta eclogites in respect to crystallization and deformation. In the eclogites no relics of an early oceanic alteration/metamorphism can be found. The plotted mineral assemblages of stage 6 refer to observations of STRECKEISEN (1928), SPAENHAUER (1932), FRAPOLLI (1975), THIERRIN (1982, 1983), KRÄHENBÜHL (1984), MICHAEL (1985). Apatite and zircon has not been drawn. Ilm = ilmenite, Mt = magnetite, Pyr = pyrite.

clusions in the core (Fig. 3b). Atoll garnets in fine grained eclogites formed around sphene-rich areas. The enclosed minerals are interpreted as relicts of an older, pre-eclogitic metamorphism. The development of the s_1 fabric indicates a penetrative deformation during a regional metamorphic event of lower amphibolite facies.

Stage 2: The parallel orientation of lance-shaped omphacite I, irregular quartz and rutile in the outer rim of the garnet core (= garnet II) denote a new foliation (Fig. 3a, d). A hiatus of growth is deduced from the observation that s_2 crosscuts s_1. This second stage was observed in a few samples only and marks the beginning of the HP overprint.

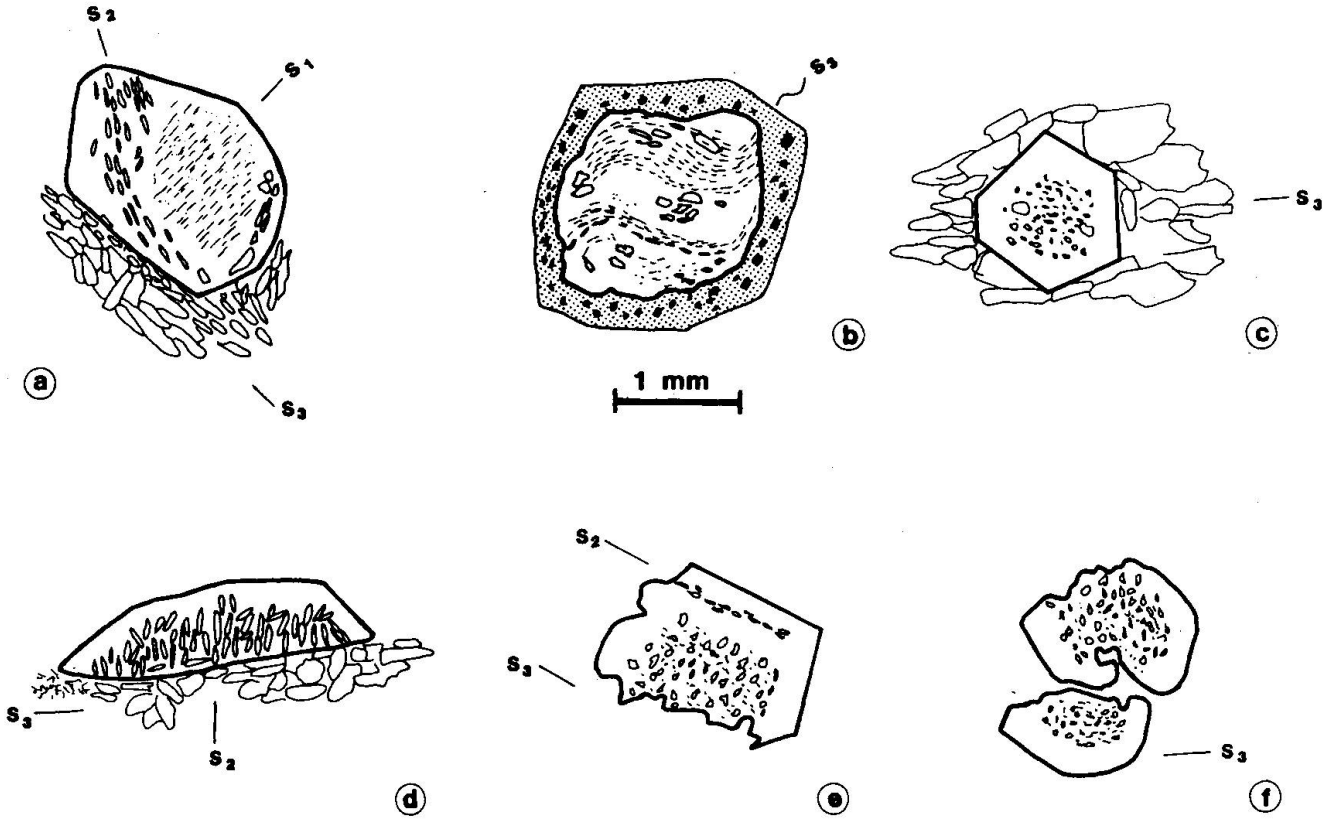

Fig. 3 Fabric relationships and mineral inclusions in porphyroblastic garnets of B-type eclogites.

a) ST 279. The inner part of the garnet core (= Garnet I) encloses clinozoisite I, Ca-amphibole I and sphene I in s_1. The outer part of the core (= Garnet II) contains predominantly omphacite I besides few rutile and zircon in s_2. The small margin is developed subhedral with few inclusions (= Garnet III). Coarser omphacite III in the matrix is aligned in s_3.

b) Ma 496. Strongly retrograde overprinted eclogite (garnet-amphibolite). A marginally kelyphitic garnet (shaded = Ca-amphibole IV and opakes) shows the rotated internal fabric of garnet I core, consisting of smallest sphene I + large Ca-amphibole I + clinozoisite I + quartz crystals in rotated s_1. S_3 too is undulated!

c) Ma 917. Euhedral garnet consists of inclusion-rich core II (inclusions: quartz, omphacite I, rutile, sphene I) and inclusion-free garnet III rim. Large matrix omphacites III are aligned in s_3.

d) ST 279. Zoned and fractured garnet composed of garnet II core with stalked omphacite II inclusions in s_2 (besides rutile and zircon) and inclusion-free garnet III rim. The matrix omphacites III which stay in contact with the garnet are aligned in s_3. Deformation D_3 already fractured the garnets, while matrix omphacites III show syntectonic recrystallization.

e) Ma 444. Deeply fractured, zoned garnet with inclusion-rich garnet I core (quartz + Ca-amphibole I + clinozoisite I + rutile + sphene I), garnet II with rutile inclusions in S_2 and subhedral garnet III rim without inclusions. Direction of S_3 in the matrix is shown.

f) Ma 444. Inclusion rich garnets were fractured and then pushed against the other. S_3 is developed in the matrix.

Stage 3: The poikiloblastic garnet I and II cores are rimmed by a subhedral border (garnet III, Fig. 3c) with only few inclusions (rutile, omphacite II, quartz). No penetrative deformation can be observed. This stage demonstrates a period of static growth of garnet III under high pressure conditions.

Stage 4: This event is characterized by a strong deformation which fractured the garnets (Fig. 3d–f). It took place under high pressure conditions because the matrix omphacites III are aligned within the penetrative schistosity s_3, the main planar element visible in hand specimens. During and/or at the final stages of this deformation large poikilitic zoisites and Ca-amphiboles II crystallized, the former being older than the latter. Their syn- to late-kinematic growth is apparent by an orientation parallel to s_3 as well as oblique to it. Their growth can only be explained by the presence at this moment of H_2O-rich and CO_2-poor fluids. In many samples, clinozoisite II replaces zoisite, but seems to have grown directly as clinozoisite. In strongly retrograded eclogites, the matrix omphacites III are replaced by symplectite of stage 5, whereas omphacite III occuring as inclusions in zoisite, clinozoisite II and/or Ca-amphibole II is unaffected by this phenomenon. Therefore the crystallization of these hydrous minerals took place prior to stage 5.

Stage 5: During this event omphacites were replaced by clinopyroxene IV + plagioclase II (An 0–3) – and/or Ca-amphibole III + plagioclase II-symplectite. Rutile is overgrown by sphene II, garnet can be replaced marginally by Ca-amphibole IV and zoisite by clinozoisite III.

Stage 6: Further recrystallization leads to the typical upper amphibolite facies association of plagioclase III (An 10–45) + Ca-amphibole V + quartz + sphene III + ilmenite/pyrite/magnetite ± clinozoisite III ± biotite ± calcite. A new penetrative schistosity s_4 is developed.

Stages 5 and 6 refer to the "retrograde" transformation of the eclogites. They are mentioned only briefly in this paper, because numerous authors (see introduction) studied the reaction products.

B-type eclogites contain quartz veins with omphacite, zoisite, rutile, apatite, Ca-amphibole and carbonate. The decay of the albite component of plagioclase I yields as reaction products the jadeite component for the omphacite as well as SiO_2 which could be dissolved in a fluid phase and crystallize as quartz-segregations parallel to the schistosity or in veins/cracks oblique to it.

2.2. MINERAL CHEMISTRY

The major minerals in the eclogites, i.e. omphacite, garnet, Ca-amphibole, zoisite and clinozoisite were analyzed in eight rock samples (mainly B-type eclogites) by microprobe at the Mineralogical Institute of the University of Bern. Omphacite I, II were not analyzed because these are not in contact with quartz or plagioclase and therefore cannot be used for P-estimations. Other minerals like white mica, biotite and plagioclase, which are present in tiny crystals only, often degraded (white micas!) or in subordinate amounts, were determined qualitatively. Analytical procedures are given by SCHWANDER and GLOOR (1980). Atomic proportions were calculated according to LAIRD and ALBEE (1981). Pyroxene and garnet atomic proportions were checked and adjusted by the method of MOTTANA (1986). The Fe^{3+} content of pyroxenes and garnets was estimated with the procedure outlined by RYBURN et al. (1976). The data set of MICHAEL (1985) is included in Fig. 4 and 6 as well as in Tab. 1 (specimen GM 18).

Omphacites: In the diagram of ESSENE and FYFE (1967) the sodic clinopyroxenes III plot in the field of omphacites (Fig. 4). The omphacites are generally homogeneous. Only coarse grains in B-type eclogites are zoned: cores contain more MgO and CaO, but less Al_2O_3 and Na_2O when compared with rims (Tab. 1, analyses 4C and 4R). Interestingly, the jadeite content of different grains in a same specimen show considerable scatter. 9 omphacites III from Ma 132, a fine grained tectonized type-A eclogite, have compositions in the range 36–59 mole% Jd! Apparently, even this rock show considerable chemical inhomogeneities on a microscale. The observed zonation in coarse omphacites III (core: Jd 34, rim: Jd 39) is indi-

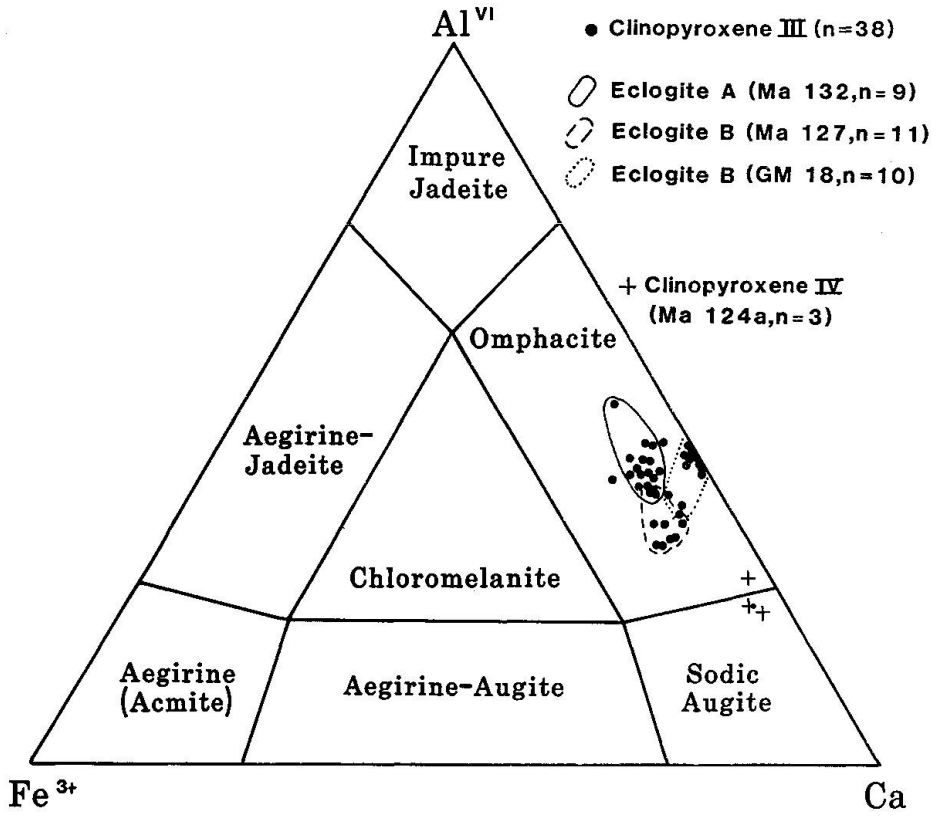

Fig. 4 Compositional diagram for clinopyroxenes (ESSENE and FYFE, 1967). The 38 clinopyroxenes III from eclogites fall within the field of omphacite, three clinopyroxenes IV from the symplectitic domains are located on the boundary to sodic augites.

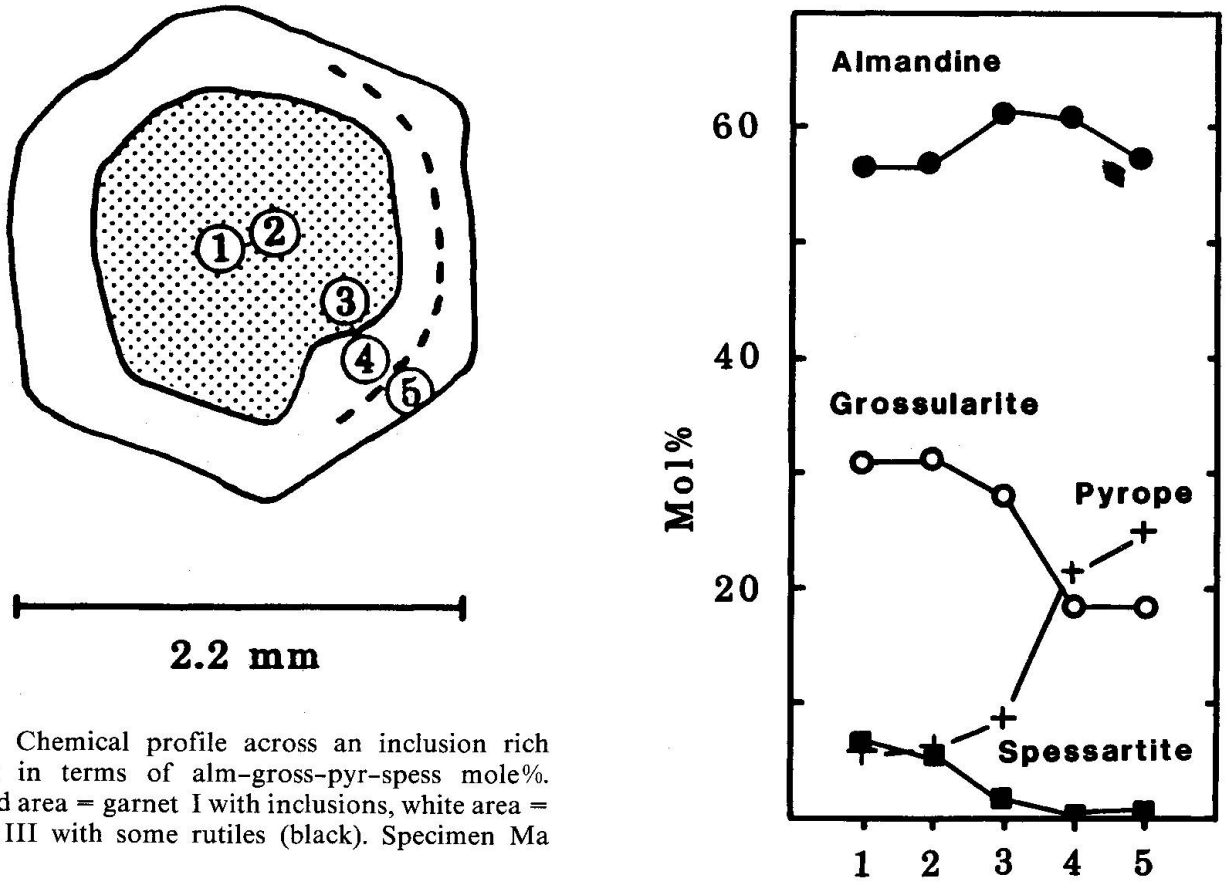

Fig. 5 Chemical profile across an inclusion rich garnet in terms of alm-gross-pyr-spess mole%. Shaded area = garnet I with inclusions, white area = garnet III with some rutiles (black). Specimen Ma 94/4.

Tab. 1 Representative electron microprobe analyses and atomic proportions (6 oxygens) for Na-clinopyroxenes III (Analyses 1-9) and IV (Analyses 10+11). C = core, R = rim. Analyses 1-3: Ma 94, 4: Ma 127, 5-7: Ma 132, 8-9: GM 18, 10-11: MA 124a.

Analysis	1	2	3	4C	4R	5	6	7	8	9	10	11
SiO_2	56.52	56.38	56.66	56.63	56.74	56.48	56.42	56.77	56.29	56.57	54.98	55.02
TiO_2	0.00	0.00	0.00	0.00	0.04	0.04	0.08	0.04	0.05	0.05	0.05	0.04
Al_2O_3	9.59	9.23	9.69	8.34	8.86	9.98	8.65	10.90	8.37	9.32	4.93	4.92
FeO_T	4.64	5.61	5.05	4.11	4.37	5.61	6.07	5.77	4.63	3.84	5.72	6.14
MnO	0.00	0.00	0.00	0.00	0.00	0.18	0.00	0.00	0.00	0.00	0.04	0.04
MgO	8.46	8.06	7.87	9.62	8.76	7.53	8.39	6.70	9.98	9.67	11.43	11.08
CaO	12.99	13.50	13.48	15.25	14.68	12.72	14.59	11.87	15.16	14.90	18.57	19.22
Na_2O	6.91	6.84	6.88	6.04	6.53	7.16	6.20	7.87	5.89	6.32	3.61	3.46
K_2O	0.00	0.00	0.00	0.00	0.00	0.00	0.01	0.00	0.00	0.00	0.00	0.00
Total	99.11	99.62	99.63	99.99	99.98	99.70	100.41	99.92	100.37	100.67	99.33	99.92
Si	2.00	2.00	2.00	2.00	2.00	2.00	2.00	2.00	2.00	2.00	2.00	2.00
Al	0.41	0.39	0.42	0.35	0.38	0.43	0.37	0.46	0.35	0.38	0.21	0.21
Fe^{2+}	0.07	0.08	0.09	0.06	0.05	0.10	0.13	0.08	0.09	0.06	0.13	0.15
Fe^{3+}	0.07	0.09	0.06	0.07	0.08	0.07	0.06	0.09	0.05	0.05	0.05	0.04
Mg	0.46	0.44	0.43	0.51	0.47	0.41	0.45	0.36	0.53	0.51	0.62	0.60
Ca	0.51	0.52	0.52	0.59	0.56	0.49	0.56	0.46	0.58	0.57	0.73	0.75
Na	0.48	0.48	0.48	0.42	0.46	0.50	0.43	0.55	0.40	0.43	0.26	0.25
Total	4.00	4.00	4.00	4.00	4.00	4.00	4.00	4.00	4.00	4.00	4.00	4.00
Jd	44	43	44	34	39	47	36	55	33	36	23	22

Tab. 2 Representative electron microprobe analyses and atomic proportions (12 oxygens) for garnets. Analyses 1-5: profile core → rim in garnet no. 4 from Ma 94 (Fig. 5), 6: Ma 127, 7: Ma 132. Garnet I: Analyses 1-3, Garnet III: Analyses 4-7. Atomic proportions (Si normalized to 3.00 and sum of the cations = 5.00) and Fe^{3+} after the method of MOTTANA (1987).

Analysis	1	2	3	4	5	6	7
SiO_2	38.00	38.77	38.98	39.62	39.18	40.37	38.99
TiO_2	0.06	0.00	0.00	0.00	0.00	0.00	0.00
Al_2O_3	20.22	21.09	21.49	21.68	21.10	21.13	21.27
FeO	25.58	26.03	28.17	28.37	26.67	23.59	25.38
MnO	2.93	2.59	0.75	0.11	0.23	0.30	0.42
MgO	1.51	1.55	2.22	5.46	6.34	7.27	3.16
CaO	11.07	10.86	10.04	6.58	6.60	8.90	11.49
Na_2O	0.03	0.04	0.00	0.00	0.03	0.00	0.05
K_2O	0.00	0.00	0.00	0.00	0.00	0.00	0.00
Total	99.40	100.93	101.65	101.82	100.15	101.56	100.76
Si	3.00	3.00	3.00	3.00	3.00	3.00	3.00
Al	1.93	1.98	1.99	1.98	1.94	1.91	1.96
Fe^{2+}	1.64	1.70	1.84	1.81	1.68	1.43	1.61
Fe^{3+}	0.08	0.03	0.01	0.02	0.06	0.09	0.05
Mn	0.20	0.17	0.05	0.01	0.01	0.02	0.03
Mg	0.18	0.18	0.26	0.63	0.75	0.84	0.37
Ca	0.96	0.93	0.85	0.55	0.55	0.73	0.97
Na	0.01	0.01	0.00	0.00	0.01	0.00	0.01

cative of prograde P,T increase due to subduction processes. The pale green pyroxenes IV from a symplectitic intergrowth with plagioclase (Tab. 1, analyses 10 and 11) are quite different. They contain more Ca and plot in the field of sodic augites (Fig. 4). Their jadeite content is low (22–23 mole%).

Garnets: Chemically the inclusion-rich cores (garnet I) differ clearly from the inclusion poor rims (garnet III), see Tab. 2. The core has less Mg (pyrope), but more Ca (grossularite) and Mn (spessartite) when compared with the subhedral rim (Fig. 5). Fig. 6 shows that the compositions of the rims are more randomly distributed than those of the cores. Garnet analyses of a fine grained A-type eclogite (Ma 132) coincide with the core compositions of garnets from B-type eclogite. Mean values for garnets from type B eclogites are:

Core (n=35, garnet I)
$Alm_{56.5}\,Spess_{2}\,Pyr_{10}\,Gross_{31.5}$

Rim (n=35, garnet III)
$Alm_{57}\,Spess_{0.5}\,Pyr_{20}\,Gross_{22.5}$

This garnet zoning is interpreted as resulting from prograde metamorphism, due to heating during subduction.

Ca-amphiboles: Selected analyses from 20 amphiboles are listed in Tab. 3. Analyses 1 and 2 belong to Ca-amphibole I, included in the inner core of garnet. Analyses 3 and 4 are specimens of Ca-amphibole II from the matrix in contact with omphacite and/or garnet. Analysis 5 is a blue-greenish amphibole IV as a rim around garnet. Analysis 6 represents a pale-green Ca-amphibole III from a coarse symplectite. These amphibole analyses plot in the field of calcic amphiboles according to LEAKE (1978). A further subdivision can be obtained on the basis of their different Al^{VI}-Si-ratio (Fig. 7). The Ca-amphibole I is similar to the matrix megacryst amphibole II and Ca-amphibole IV. Ca-amphibole II are generally zoned

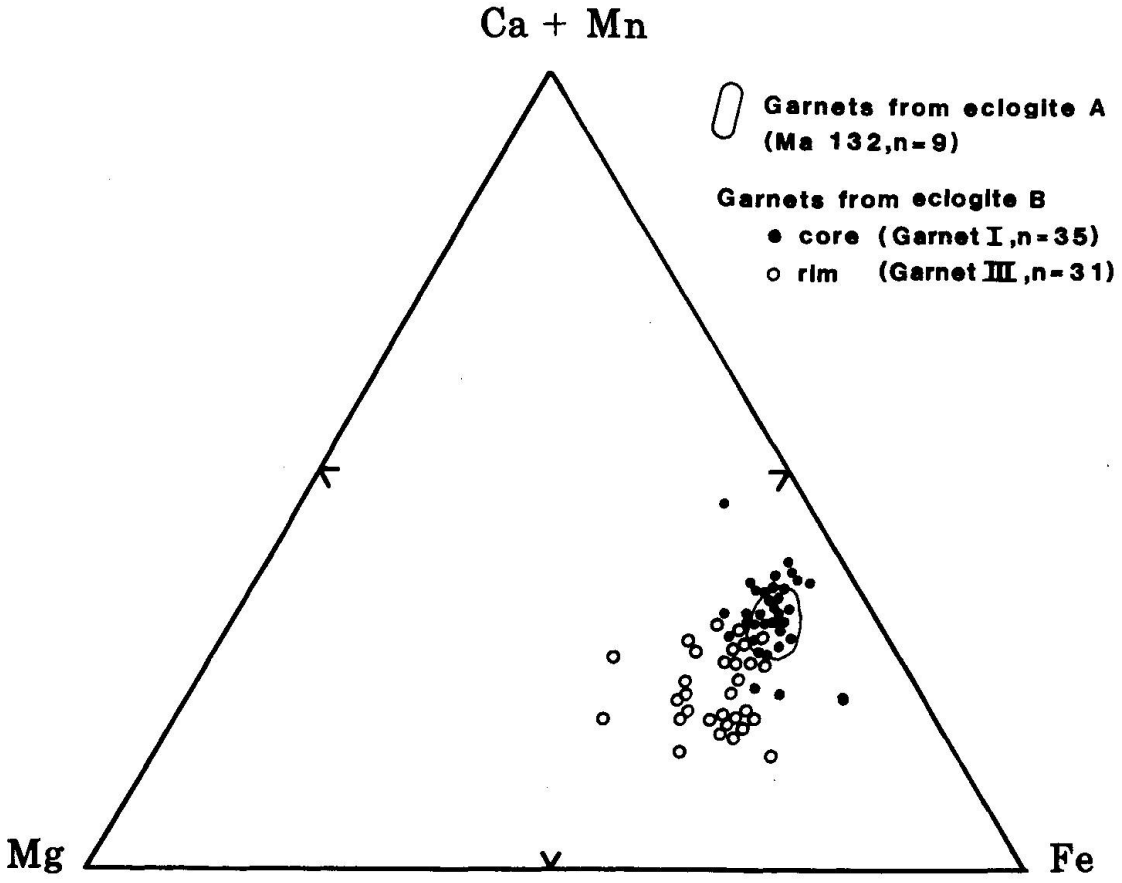

Fig. 6 Ternary diagram Mg–Ca+Mn–Fe^{2+} for garnets.

Tab. 3 Representative electron microprobe analyses and atomic proportions (23 oxygens) for amphiboles. C = core, R = rim. Analyses 1+4+6: Ma 124e, 2+5: Ma 124a, 3: Ma 130.

Analysis	1	2	3C	3R	4	5	6
SiO_2	43.93	44.03	52.43	52.20	44.88	43.65	45.20
TiO_2	0.55	0.71	0.08	0.10	0.40	0.21	0.52
Al_2O_3	14.84	15.51	6.52	6.59	12.80	14.40	12.70
FeO_T	13.10	15.26	9.88	9.10	12.87	17.80	11.26
MnO	0.10	0.06	0.05	0.06	0.00	0.14	0.00
MgO	12.15	8.89	16.92	16.71	13.42	8.71	15.00
CaO	8.90	9.03	8.88	8.96	8.32	9.18	9.10
Na_2O	4.33	4.51	3.30	3.23	4.70	3.78	4.38
K_2O	0.27	0.33	0.21	0.25	0.36	0.56	0.35
Total	98.17	98.33	98.27	97.20	97.75	98.43	98.51
Si	6.39	6.45	7.40	7.42	6.55	6.48	6.51
Al^{IV}	1.60	1.54	0.59	0.57	1.44	1.52	1.48
Al^{VI}	0.94	1.14	0.49	0.53	0.76	1.00	0.67
Ti	0.06	0.07	0.01	0.01	0.04	0.07	0.05
Fe^{2+}	1.59	1.87	1.16	1.08	1.57	1.87	1.35
Mn	0.01	0.01	0.01	0.01	0.00	0.01	0.00
Mg	2.63	1.94	3.56	3.54	2.92	1.94	3.22
Ca	1.38	1.41	1.34	1.36	1.30	1.46	1.40
Na	1.22	1.28	0.90	0.89	1.33	1.08	1.22
K	0.05	0.06	0.03	0.04	0.06	0.10	0.06
Total	15.87	15.77	15.49	15.45	15.97	15.53	15.90

Tab. 4 Representative microprobe analyses and atomic proportions (12 oxygens) of zoisites (Analyses 1+2: Ma 277) and clinozoisites (Analyses 3+4: Ma 127).

Analysis	1	2	3	4
SiO_2	40.09	39.78	39.58	39.59
TiO_2	0.00	0.00	0.13	0.16
Al_2O_3	31.57	30.84	29.70	27.83
FeO	1.96	2.67	4.93	5.58
MnO	0.00	0.00	0.00	0.00
MgO	0.00	0.00	0.00	0.12
CaO	24.51	24.29	24.17	24.04
Na_2O	0.00	0.00	0.00	0.00
K_2O	0.00	0.00	0.00	0.00
Total	98.13	97.58	98.51	97.32
Si	2.93	2.94	2.93	2.98
Ti	0.00	0.00	0.01	0.01
Al	2.72	2.68	2.59	2.47
Fe^{2+}	0.12	0.16	0.30	0.35
Ca	1.92	1.92	1.91	1.94
Total	7.69	7.70	7.74	7.75

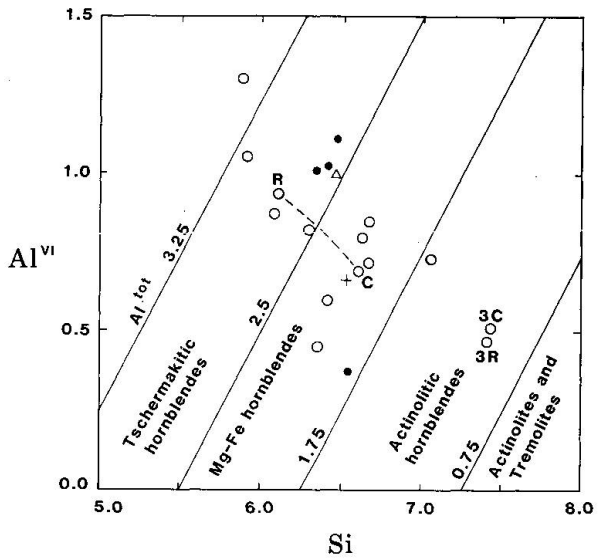

Fig. 7 Compositional variation of Ca-amphiboles in a Al^{VI} vs. Si diagram (LEAKE, 1978). Dot: Ca-amphibole I, circle: Ca-amphibole II, cross: Ca-amphibole III, triangle: Ca-amphibole IV. C = core, R = rim.

(Fig. 7), but homogeneous actinolitic varieties also occur (Tab. 3 + Fig. 7, analyses 3C and 3R).

Zoisites/Clinozoisites: Zoisites are quite homogeneous and have higher Al_2O_3 but lower FeO content in comparison to clinozoisites (Tab. 4, Fig. 8). The latter show marked inhomogeneities due to changing Al/Fe ratios (Fig. 8, 9).

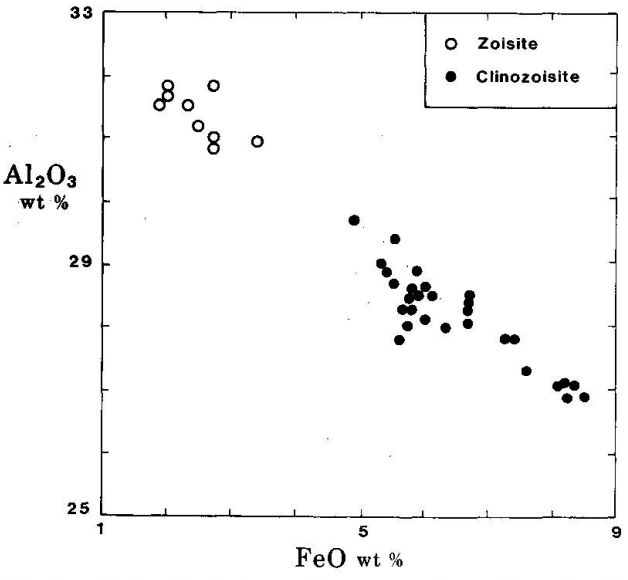

Fig. 8 Al_2O_3-FeO plot of 9 spot analyses from 2 zoisites and 29 spot analyses from 6 individual clinozoisite II grains (specimens Ma 124e, 127, 130 and 277). All grains as individuals in the matrix.

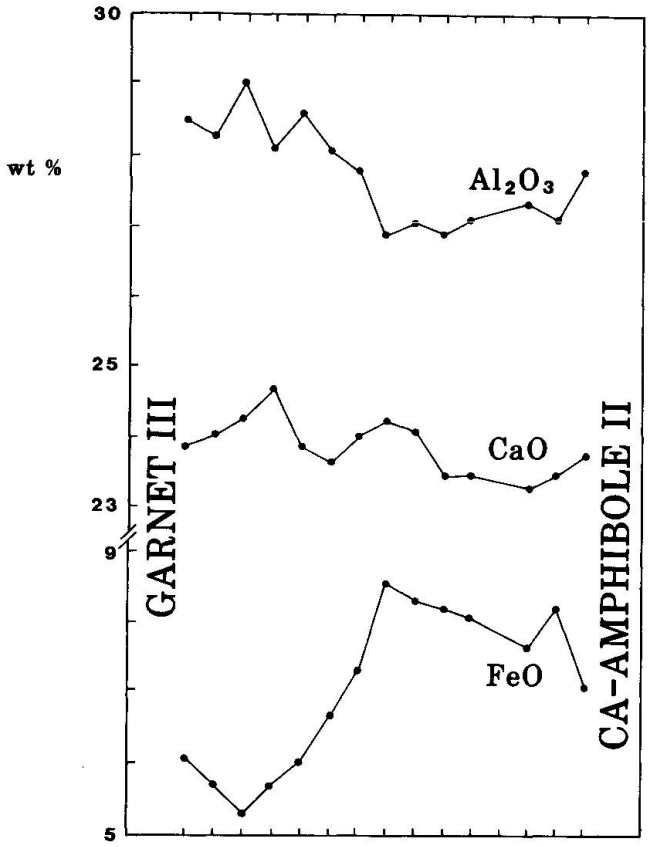

Fig. 9 Microprobe profile through a clinozoisite II bordered by a garnet III and a Ca-amphibole II (clinozoisite 3 of specimen Ma 130). Each bar on the horizontal scale = 10 microns. Note the strong variations in FeO and Al_2O_3.

2.3. T, P CONDITIONS OF THE HP EVENT

Temperature: The absence of glaucophane indicates a minimum temperature of 500 °C (MARESCH, 1977). As chemical zoning only develops at temperatures below 650–700 °C (e.g. TRACY, 1982), this should be the maximum temperature for most B-type eclogites. Further limits of the temperature range are obtained with the garnet-omphacite geothermometer (ELLIS and Green, 1979). Non-equilibrium conditions for contact pairs of B-type eclogites are reflected by the wide range of the K_D's (12–45, Fig. 10a) leading to irrealistic T-estimations (Fig. 10b). Contrasting, contact pairs from A-type eclogites have less scattered K_D's (14–30, Fig. 10a). Equilibrium temperatures of 540–630 °C can be inferred for assumed 10–15 kb (Fig. 10b).

Pressure: This parameter was estimated with the albite = jadeite + quartz barometer

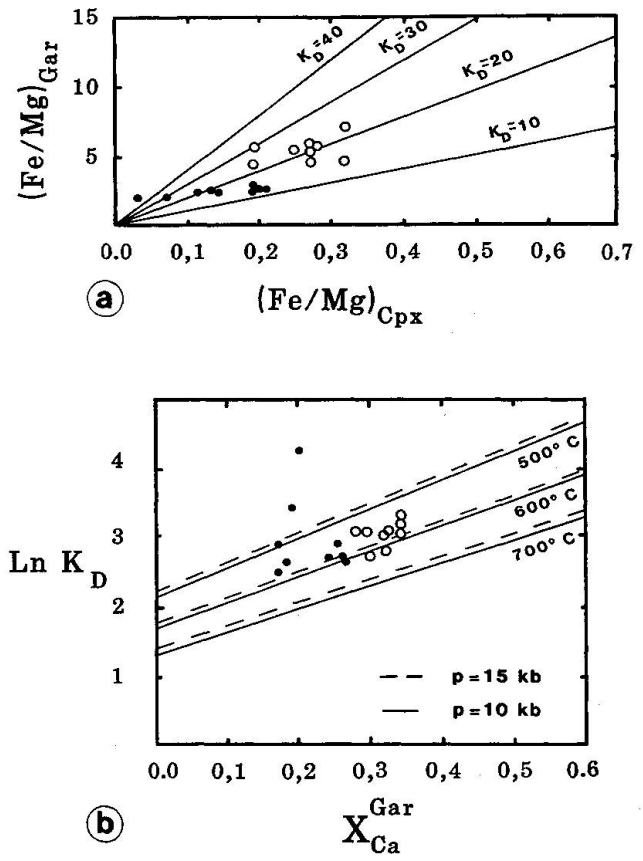

Fig. 10

a) Distribution of analyzed garnet/omphacite pairs on a $(Fe/Mg)_{Gar}$ vs. $(Fe/Mg)_{Cpx}$ diagram for fine-grained equilibrium eclogite A (circles, Ma 132) and for non-equilibrium eclogites B (dots; Ma 94, Ma 127).

b) Variation of calculated $\ln K_D$ with X_{Ca}^{Gar} in "coexisting" garnet-omphacite pairs at 10 and 15 kb pressure for the temperature range 500–700 °C. The straight lines have been calculated according to the experiments of ELLIS and GREEN (1979).

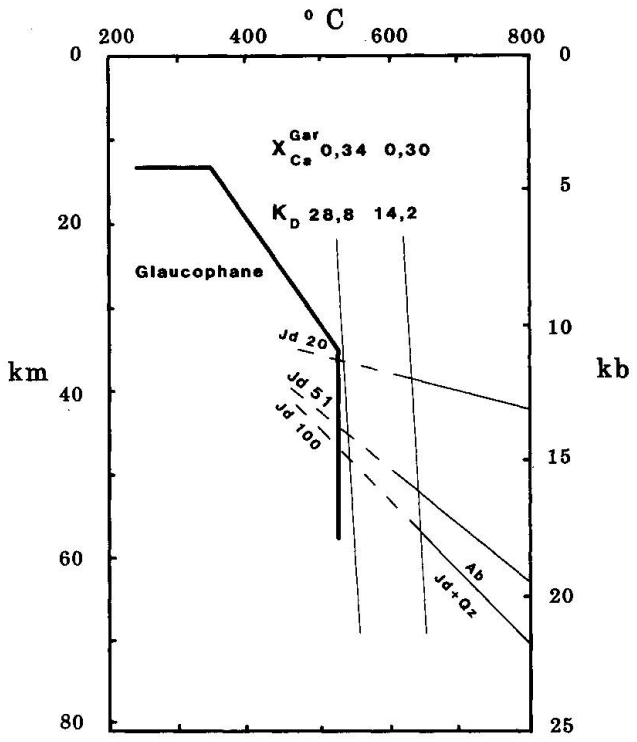

Fig. 11 P-T diagram for the estimation of the P, T conditions of the eclogite metamorphism. The equilibria shown are: the stability field of glaucophane according to MARESCH (1977), the stability curves of omphacite coexisting with quartz and albite (GASPARIK and LINDSLEY, 1980), the Fe-Mg fractionation trends in garnet-clinopyroxene pairs from equilibrium eclogite A (Ma 132, maximum and minimum K_D values) calculated with the ELLIS and GREEN (1979) equation.

(NEWTON and SMITH, 1967; HOLLAND, 1980). The highest jadeite content of omphacite from a contact pair in the equilibrium eclogite Ma 132 is at 51 mole%. The K_D values in this sample vary from 14.2 to 28.8. The point of intersection of the Jd 51 curve (GASPARIK and LINDSLEY, 1980) with these two curves results in minimum pressures of 14–16 kb and temperatures of 550–650 °C for this specimen (paragenesis: omphacite + garnet + quartz + rutile, Fig. 11), corresponding to a depth of about 45–53 km. The maximum pressure can not be evaluated, as omphacite is not in equilibrium with plagioclase during the eclogitic episode. Unfortunately, the white micas could not be analyzed due to their secondary degradation.

3. Magmatic petrology

A detailed geochemical study of 67 eclogite samples (MAGGETTI et al., 1987) established the orthogenic, tholeiitic and co-magmatic nature of the protoliths. They discussed primarily the geotectonic position of the precursor rocks. In this chapter, the magmatic history will be considered in more detail.

3.1. FRACTIONATION EFFECTS

Any discussion about basaltic fractionation has to be based primarily on aphyric or glassy rocks representing former liquids. However, when metamorphosed, such rocks are not easily detected! PEARCE (1983a) proposed an Al_2O_3/TiO_2-screen to separate cumulates from

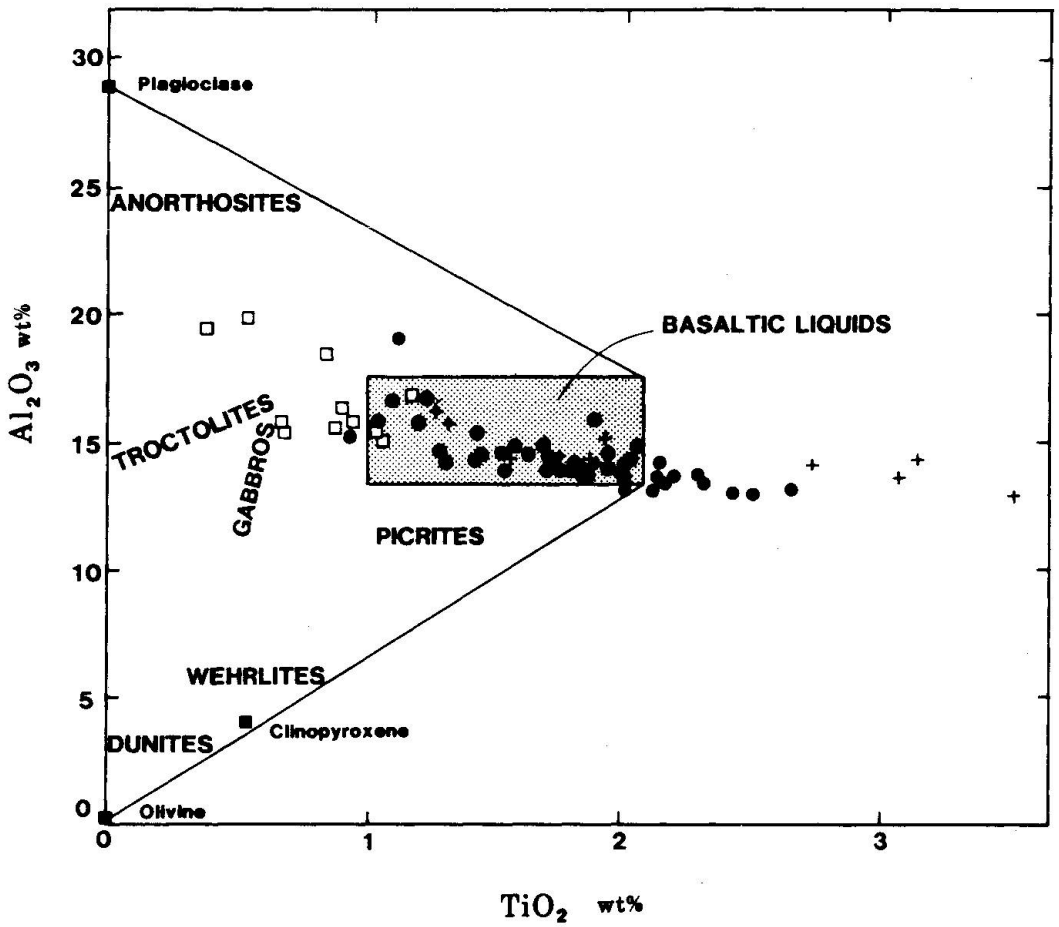

Fig. 12 Selection of "basaltic liquids" in a Al_2O_3/TiO_2 plot (PEARCE, 1983a). Symbols as used by MAGGETTI et al., 1987); open squares = eclogite 1, dots = eclogite 2, crosses = eclogite 3.

true basaltic liquids. If this method is used for the 67 samples, only 42 appear to have approximate basaltic compositions (Fig. 12).

Primitive basaltic, non cumulative magmas are characterized by mg-numbers 0.70–0.75 and Ni 200–450 ppm (B.V.S.P. 1981). The least evolved eclogite protoliths have mg-numbers between 0.58 and 0.60 and Ni contents between 57 and 126 ppm. Therefore these rocks do not correspond to primitive mantle derived melts, but are differentiation products of such melts. Plots of "immobile" major elements against a parameter of igneous differentiation, e.g. mg-number (Fig. 13) reveal good positive or negative correlations. These reflect strong fractional crystallization controls. The eclogite data have clear affinities to modern evolved MORB glasses. The parallel alignment of the Silvretta trend with the one of the MORB glasses (Fig. 13a) shows that olivine + plagioclase + clinopyroxene fractionation could have controlled the evolution of the eclogite precursor liquids (B.V.S.P. 1981). In contrast to MORB glasses, the shift of the Silvretta data is probably caused by a different chemical composition of their mantle sources. With advancing fractionation the Fe-enrichment trend (Fig. 13b) characterizes tholeiitic series (MIYASHIRO, 1975) and leads to ferro-basaltic residual liquids. In Fig. 13c, the Silvretta data occupy the MORB glass field, which defines a low pressure liquid line of descent. Ocean ridge basalts differentiate along this line by simultaneous crystallization of olivine + plagioclase (+ clinopyroxene). The observed trends of Ca-, Mg-, Ni- and Cr-depletion as well as the negative Eu-anomalies in chondrite-normalized REE patterns (MAGGETTI et al., 1987) are consistent with such a fractionation scheme. These patterns involve perhaps some removal of a Cr-spinel at an earlier stage of differentiation. Removal of apatite (no P-depletion), amphibole (no Nb-, Ti-, Y-depletion) or garnet (no Y-depletion) is not indicated. Therefore, fractionation of the eclogite protoliths at great depths can be excluded.

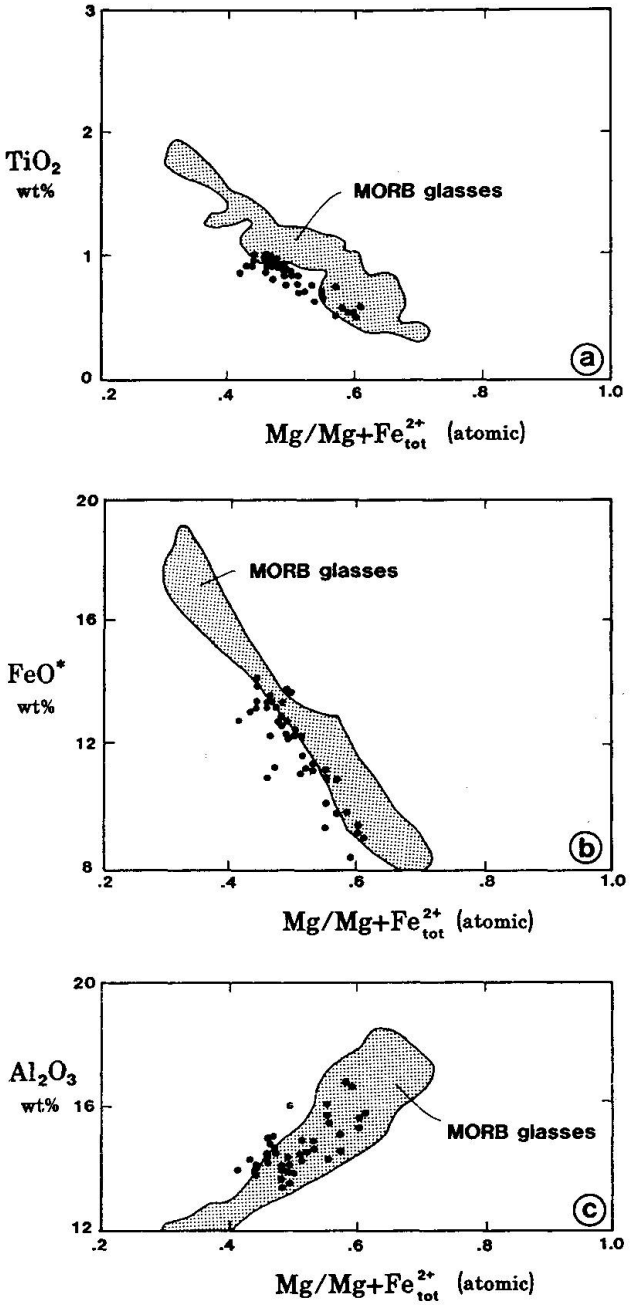

Fig. 13 42 "basaltic liquid" (PEARCE, 1983a) analyses of eclogitic rocks from the Silvretta showing the incompatible behaviour of TiO_2 (a) and FeO* (b) and the compatible nature of Al_2O_3 (c) when plotted against a differentiation index like the mg-number. FeO* = total Fe as FeO. Field of MORB glasses according to B.V.S.P. (1981).

The chemical composition of the eclogites is consistent with their production at crustal levels in shallow magma chambers (< 5–6 kb, KUSHIRO, 1973; GREEN, 1982) by low pressure tholeiitic fractionation of the inferred liquidus or near liquidus phases olivine + Cr-spinel + plagioclase + clinopyroxene. Such processes are known to occur at accreting plate margins under reduced pH_2O-fO_2 conditions (HILL and ROEDER, 1974; MORSE et al., 1980). Removal of these phases caused rapid depletion of Mg, Ca, Ni and Cr and gave rise to the increase of Fe, Ti and other incompatible elements such as P, Zr and Y.

3.2. CONTAMINATION VS. POSTMAGMATIC EFFECTS

In a co-magmatic series that is related by fractional crystallization processes of a common magma, the chemical elements should behave compatibly or incompatibly (e.g. arranged on negative or positive vectors when plotted against an incompatible element like Zr). According to MAGGETTI et al. (1987) this holds for many elements, but Si, K, Na, Sr, Ba, Zn and Cu are irregularly scattered. This can be explained either by contamination by crustal materials during ascent/crystallization or by post-magmatic alterations due to weathering and/or metamorphism.

The effects of such open-system processes can be detected with a rock/MORB normalized diagram (Fig. 14). Sample Ma 414, which

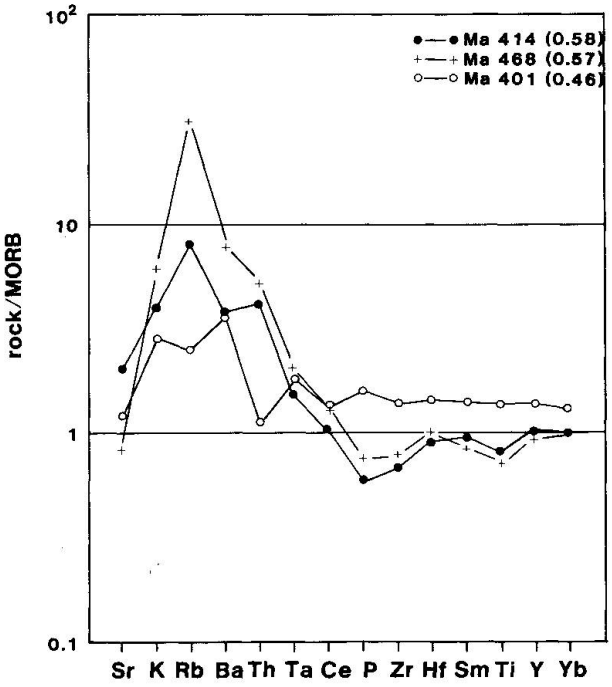

Fig. 14 Rock/MORB plot of three selected eclogites. Normalization factors from PEARCE (1983b). Numbers in parantheses = mg-number.

is the least evolved basic magma of the "basaltic" eclogite set (Cr: 444, Ni: 126, Y: 30 ppm) and Ma 468, a slightly more evolved basic liquid (Cr: 236, Ni: 73, Y: 29 ppm) are enriched in Sr, K, Rb, Ba, Th, Ta and depleted in the other elements. A more differentiated liquid like Ma 401 (Cr: 109, Ni: 59, Y: 42 ppm) shows an identical shape of pattern. The strongly enriched behaviour shown on the left side of the diagram can be explained by contamination or alteration effects. If contamination was operating, the least evolved liquids should show a less enriched pattern whereas subsequently more evolved liquids which were exposed to contamination during a greater laps of time should have stronger enrichment. The three examples do not show such an expected, regular vertical shifting – on the contrary, the most evolved liquid has the least enriched pattern. Therefore, the observed arrangement can best be explained by post-magmatic alterations. The absence of any Ce-depletion (MASUDO and NAGASAWA, 1975; HELLMANN and HENDERSON, 1977; HELLMANN et al.,1977; LUDDEN and THOMPSON, 1979) indicates that the mobilization of this element and the other mentioned above did not occur during a low grade overprint, but more likely at a higher grade. Mobility of these elements is attested by the high-pressure segregations (quartz veins with HP-minerals) discussed in the previous section.

3.3. GEODYNAMIC INTERPRETATION

MAGGETTI and GALETTI (1984) and MAGGETTI et al. (1987) placed the chemical features of the eclogites of the Silvretta in a geotectonic framework. They established MORB-affinities for most of the samples, with some indications of an IAB-origin (mostly eclogite-3 types). Therefore, the authors postulated a generation of the eclogite precursor rocks in a dominantly divergent and subordinate convergent plate margin (e.g. back arc basin) setting.

However, the Al_2O_3/TiO_2 filter shows that the presumed IAB-protoliths are cumulates! They can therefore not be used for the interpretation of the original geotectonic environment. A much more coherent interpretation is obtained, if only the 42 "basaltic liquid" analyses are considered. Immobile incompatible element ratios such as V/Ti (Fig. 15a) or Ti/Zr (Fig. 15b) plot well within the range shown by ridge-generated basalts. The same geotectonic settings appear in Fig. 15c and 15d. Chondrite-normalized REE-patterns are mostly flat to LREE-enriched like T-type MORB or have the LREE-depleted slopes typical of N-type MORB. Serpentinite bodies (CADISCH et al., 1941; BRÖCKER, 1985; FUCHS et al., 1986) as well as the presence of gabbros and ultramafic cumulates in the Silvretta metabasites combined with the observed marked Ti- and Fe-enrichment trends of the liquid compositions are consistent with a magmatic evolution in small magma chambers under an oceanic ridge. An ophiolitic nature can therefore be postulated. Detritic metasediments are closely associated with the metabasic units. In case of a primary nature of these associations, both petrogenetic and lithostratigraphic arguments seem to hold for a model with an incipient oceanic rift operating after continental breakup and lithospheric thinning. Jurassic examples of such settings were presented by BECCALUVA et al. (1984).

4. Genesis of the Silvretta eclogites: a possible history

Based upon the results of the previous chapters, the following evolution path of the Silvretta eclogites is suggested (Fig. 16):

I. Igneous episode: Crystallization of protoliths as oceanic extrusions/intrusions of tholeiitic affinities with distinct differentiation characteristics. No igneous minerals preserved. Age of crystallization unknown. Geotectonic setting: constructive plate margin, near to a continent. No relics of a subsequent oceanic metamorphism.

II. Metamorphism 1 (Stage 1 of Fig. 2): Ductile deformation under amphibolite facies conditions leads to the formation of s_1 (relicts in garnet cores). P, T conditions (Ca-amphibole I indicate T > 500 °C) and age unknown.

III. Metamorphism 2 (Stages 2–4): High pressure event with complicated deformation/crystallization phases. Coarse eclogites show several generations of garnet and omphacite. P,T conditions of the last deformation D3, overprinting all other fabrics are estimated as minimum pressures of 14–16 kb and tempera-

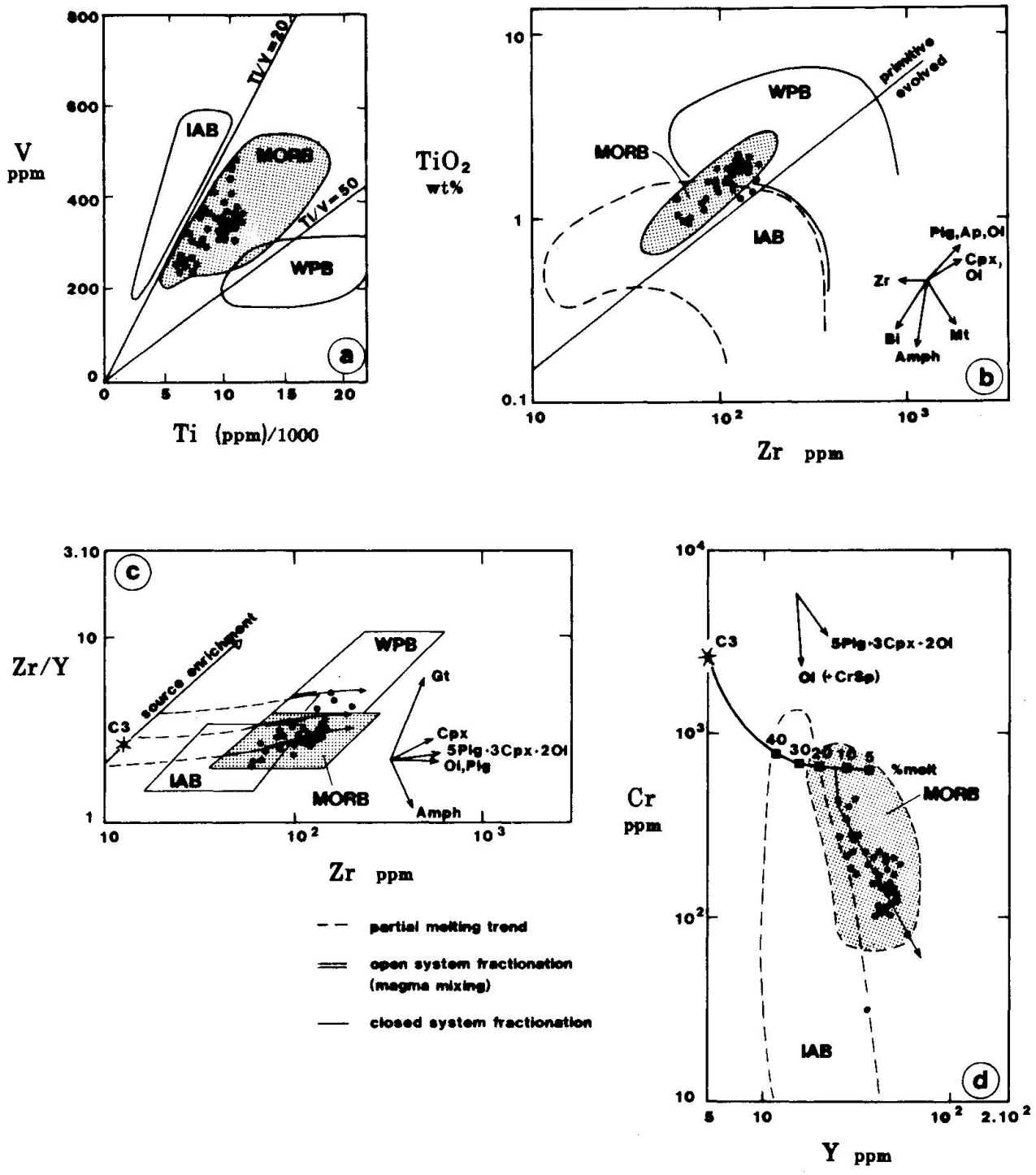

Fig. 15 a) V-Ti/1000 plot (SHERVAIS, 1982; HODDER, 1985). The 42 eclogite analyses corresponding to basaltic liquids cluster in the fields of mid-ocean ridge basalts (MORB). IAB = island arc basalt, WPB = within plate basalts.

b) TiO_2-Zr diagram (PEARCE and CANN, 1973). The 42 eclogite analyses fall well within the fields of MORB. Differentiation trends for specific minerals are shown.

c) Zr/Y-Zr diagram (PEARCE and NORRY, 1979). 42 eclogite analyses plot almost all in the MORB field. Fractionation trends of specific mineral assemblages are shown. C3 = plagioclase-lherzolite source.

d) Cr-Y plot (PEARCE, 1980). A partial melting curve of a plagioclase-lherzolite (C3) source and fractionation trends are given. About 10–20% melting is suggested to produce the primary magmas for the protolith generation.

tures of 550–650 °C. Geotectonic setting: destructive plate margin (subduction zone). Age unknown.

IV. Metamorphism 3 (Stage 5): Isothermal (?) pressure release results in "retrograde" overprint of omphacite by symplectitic intergrowth. The coexistence of plagioclase + clinopyroxene (Jd 20) allows pressure estimate of 12–13 kb for assumed temperatures of 550–650 °C. Age unknown.

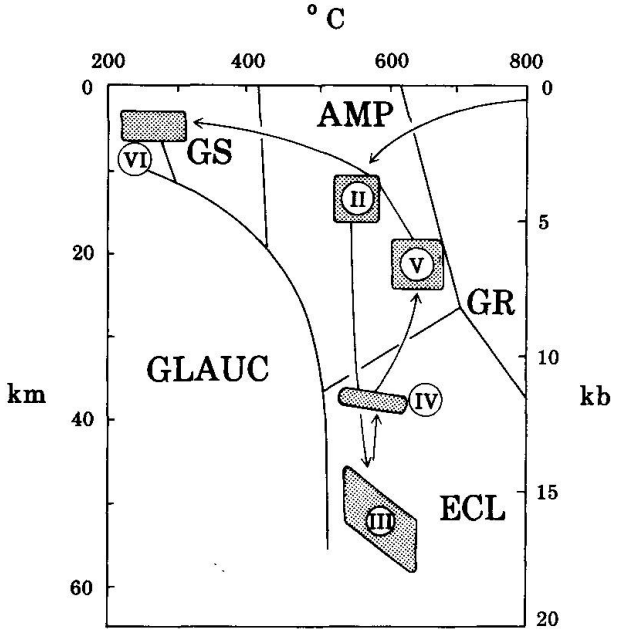

Fig. 16 Estimated P-T paths for the Silvretta eclogites from extrusion (Episode I, not shown, T ~ 1100 °C) to Alpine metamorphism (Episode VI). Simplified petrogenetic grid after MARESCH (1977) and ERNST (1981). AMP = amphibolite facies, ECL = eclogite facies, GLAUC = glaucophane facies, GR = granulite facies, GS = greenschist facies. See text for further explanations.

V. Metamorphism 4 (Stage 6): It is unknown whether the recrystallization (amphibolite facies conditions) occurred immediately after metamorphism 3 or if the rocks had a more complicated path in the P,T diagram. This overprint could be Variscan (370–350 Ma for the peak, FLISCH, 1987) or polymetamorphic including older (Pan-african) amphibolite facies metamorphism. The pressure and temperature were estimated by several authors (FRAPOLLI, 1975; FLISCH, 1981; THIERRIN, 1982, 1983; KRÄHENBÜHL, 1984; BRÖCKER, 1985; MICHAEL, 1985, 1986) to range between 5–7 kb and 550–650 °C. The estimation of FLISCH (1987), i.e. 5,5–7,5 kb/600–680 °C for the Hercynian metamorphic peak are shown in Fig. 16. For clarity, the subsequent Variscan P,T path as postulated by FLISCH (1987) has been omitted.

VI. Metamorphism 5: A last mainly brittle deformation of Eo-alpine age (110 Ma, FLISCH, 1986) affected the eclogites under anchimetamorphic to greenschist facies conditions (P: max. 1–2 kb, T: max. 175–300 °C; THÖNI, 1981, 1982, 1983; FLISCH, 1986, 1987).

Acknowledgments

This work was supported by the Swiss National Foundation (grants 2.920-0.83 and 2.856-0.85). Thanks are due to: Marco, Pascal and Simon for the help in field work, O. Marbacher for assistance in laboratory work, J.P. Bourqui for the confection of the thin sections, R. Oberhänsli for his patience with the senior author during microprobe work, B. Hellermann for the translation of a first version, J. Charrière and B. Hellermann for the drawings, M. Zingg for the copy of the report of Pearce (1983a) and G. Piller for the typing of the manuscript. The final presentation of this paper was markedly improved by critical comments of the reviewers V. Dietrich and C. Miller.

References

BEARTH, P. (1932a): Die Diabasgänge der Silvretta. Schweiz. Mineral. Petrogr. Mitt., 12, 147–178.

BEARTH, P. (1932b): Geologie und Petrographie der Keschgruppe. Schweiz. Mineral. Petrogr. Mitt., 12, 256–278.

BECCALUVA, L., DAL PIAZ, G.V. and MACCIOTTA, G. (1984): Transitional to normal MORB affinities in ophiolitic metabasites from the Zermatt, Saas, Combin and Antrona units, Western Alps: Implications for the Paleogeographic evolution of the Western Tethyan Basin. Geologie en Mijnbouw, 165–177.

BRÖCKER, M. (1985): Petrographische und geochemische Untersuchungen im Val Tuoi (Silvretta, Schweiz). Diploma, University of Tübingen, Tübingen (unpublished).

B.V.S.P. (BASALTIC VOLCANISM STUDY PROJECT) (1981): Basaltic Volcanism on the Terrestrial Planets. Pergamon, New York, N.Y., 1286 pp.

CADISCH, J., BEARTH, P. and SPAENHAUER, F. (1941): Erläuterungen zum Geologischen Atlas der Schweiz 1:25000, Blatt 420 Ardez. Geol. Kommission Schweiz. Natf. Ges., Francke, Bern.

ELLIS, D.J. and GREEN, D.H. (1979): An experimental study of the effect of Ca upon garnet-clinopyroxene Fe-Mg exchange equilibria. Contrib. Mineral. Petrol. 71, 13–22.

ERNST, W.G. (1981): Petrogenesis of eclogites and peridotites from the Western and Ligurian Alps. Am. Min. 66, 443-472.

ESSENE, E.J. and FYFE, W.S. (1967): Omphacites in Californian metamorphic rocks. Contrib. Mineral. Petrol., 15, 1-21.

FLISCH, M. (1981): Geologie und Petrographie der Rotbüelgruppe. Liz. Thesis, Universität Bern (unpublished).

FLISCH, M. (1986): Die Hebungsgeschichte der oberost-alpinen Silvretta-Decke seit der mittleren Kreide. Bull. Ver. Schweiz. Petr.-Geol. Ing., 53(123), 23-49.

FLISCH, M. (1987): Teil 1: Geologische, petrographische und isotopengeologische Untersuchungen an Gesteinen des Silvrettakristallins. Teil 2: Die Hebungsgeschichte der oberostalpinen Silvretta-Decke seit der mittleren Kreide. Teil 3: K-Ar Dating of Quaternary Samples. Thesis, Universität Bern (unpublished).

FRAPOLLI, G. (1975): Petrografia della regione del passo della Flüela. Schweiz. Mineral. Petrogr. Mitt., 55, 307-364.

FUCHS, G., KURAT, G. and NTAFLOS, T. (1986): Ein Peridotit-Vorkommen im Silvretta-Kristallin südlich von Galtür. Jb. Geol. B.-A., 129, 2, 283-290.

GASPARIK, T. and LINDSLEY, D.H. (1980): Phase equilibria at high pressure of pyroxenes containing monovalent and trivalent ions. In: PREWITT, C.T. (ed.): Pyroxenes. Reviews in Mineralogy 7, Min. Soc. America, 309-336.

GREEN, D.H. (1982): Anatexis of mafic crust and high pressure crystallization of andesite. In THORPE, R.S. (ed.): Andesites. Wiley and Sons, New York, 466-487.

HELLMANN, P.C. and HENDERSON, P. (1977): Are rare earth elements mobile during spilitization? Nature, 267, 38-40.

HELLMANN, P.C., SMITH, R.E. and HENDERSON, P. (1977): Rare earth element investigation of the Chiefdon outcrop, N.S.W. Australia. Contrib. Mineral. Petrol., 65, 155-164.

HILL, R. and ROEDER, P. (1974): The crystallization of spinel from basic liquid as a function of oxygen fugacity. J. Geol., 82, 709-729.

HODDER, A.P.W. (1985): Depth of origin of basalts inferred from Ti/V ratios and a comparison with the K_2O-depth relationship for island-arc volcanics. Chem. Geol., 48, 3-16.

HOERNES, S. (1971): Petrographische Untersuchungen an Paragneisen des polymetamorphen Silvretta-Kristallins. Tschermaks Mineral. Petrogr. Mitt., 15, 56-70.

HOLLAND, T.J.B. (1980): The reaction albite = jadeite + quartz determined experimentally in the range 600-1200°C. Amer. Min., 65, 129-134.

KRÄHENBÜHL, R. (1984): Petrographisch-geologische Untersuchungen in der Silvretta-Masse vom Flüela-Weisshorn zu Gorihorn und Rosställispitz (Kanton Graubünden). Liz. Thesis, Universität Bern (unpublished).

KUSHIRO, I. (1973): Origin of some magmas in oceanic and circum-oceanic regions.Tectonophysics, 17, 211-222.

LAIRD, J. and ALBEE, A.L. (1981): High pressure metamorphism in mafic schist from northern Vermont. Am. J. Sci., 281, 97-126.

LEAKE, B.E. (1978): Nomenclature of amphiboles. Am. Mineral., 63, 1023-1052.

LUDDEN, J.N. and THOMPSON, G. (1979): An evaluation of the behaviour of the rare earth elements during weathering of sea-floor basalt. Earth Planet. Sci. Lett., 43, 85-92.

MAGGETTI, M. und GALETTI, G. (1984): Chemie und geotektonische Position von Metabasiten aus dem Südosten der Silvretta (Schweiz). Schweiz. Mineral. Petrogr. Mitt., 64, 423-450.

MAGGETTI, M., GALETTI, G. and STOSCH, H.-G. (1987): Eclogites from the Silvretta Nappe (Switzerland): Geochemical constraints on the nature and geotectonic setting of their protoliths. Chem. Geol., 64, 319-334.

MARESCH, W.G. (1977): Experimental studies on glaucophane: an analysis of present knowledge. Tectonophysics, 43, 109-125.

MASUDO, A. and NAGASAWA, S. (1975): Rocks with negative Cerium anomalies dredged from the Skatsky Rise. Geochem. J., 9, 227-233.

MICHAEL, G. (1985): Geologie and Petrographie im Macun (Unterengadin). Diploma, Universität Fribourg (unpublished).

MICHAEL, G. (1986): Geologie und Petrographie im Macun (Unterengadin). Nachrichten der Schweiz. mineral. petrogr. Ges., Nov. 1986.

MIYASHIRO, A. (1975): Classification, characteristics and origin of ophiolites. J. Geol., 83, 249-281.

MORSE, S.A., LINDSLEY, D.H. and WILLIAMS, R.J. (1980): Concerning intensive parameters in the Skaergaard intrusion. Am. J. Sci., 280 (A), 159-170.

MOTTANA, A. (1986): Crystal-chemical evaluation of garnet and omphacite microprobe analyses: Its bearing on the classification of eclogites. Lithos, 19, 171-186.

NEWTON, R.C. and SMITH, J.V. (1967): Investigations concerning the breakdown of albite at depths in the earth. J. Geol., 75, 236-268.

PEARCE, J.A. (1980): Geochemical evidence for the genesis and eruptive setting of lavas from Tethyan ophiolites. In: PANAYIOTOU, A. (ed). Proc. int. Ophiolite Conference, Nicosia, Cyprus, 261-272.

PEARCE, J.A. (1983a): A "users guide" to basalt discrimination diagrams. Unpubl. Report, The Open University, Milton Keynes, 37 p.

PEARCE, J.A. (1983b): Role of the Sub-continental Lithosphere in Magma Genesis at Active Continental Margins. In: C.J. HAWKESWORTH and M.J. NORRY (eds): Continental Basalts and Mantle Xenoliths, Shiva Geology Series, 230-249.

PEARCE, J.A. and CANN, J. (1973): Tectonic setting of basic volcanic rocks determined using trace element analysis. Earth Planet. Sci. Lett., 19, 290-300.

PEARCE, J.A. and NORRY, M.J. (1979): Petrogenetic implications of Ti, Zr, Y and Nb variations in volcanic rocks. Contrib. Mineral. Petrol., 69, 33-47.

RYBURN, R.J., RÅHEIM, A. and GREEN, D.H. (1976): Determination of P,T paths of natural eclogites during metamorphism: record of subduction. Lithos, 9, 161-164.

SCHWANDER, H. and GLOOR, F. (1980): Zur quantita-

tiven Mikrosondenanalyse von geologischen Proben mittels kombiniertem EDS-WDS. X-ray Spectrometry, 9, 3, 134-137.

SHERVAIS, J. W. (1982): Ti-V plots and the petrogenesis of modern and ophiolitic lavas. Earth Planet. Sci. Lett., 59, 101-118.

SPAENHAUER, E. (1932): Petrographie und Geologie der Grialetsch-Vadret-Sarsura-Gruppe. Schweiz. Mineral. Petrogr. Mitt., 12, 27-146.

SPITZ, A. and DYHRENFURTH, G. (1914): Monographie der Engadiner Dolomiten zwischen Schuls, Scanfs und dem Stilfserjoch. Beitr. Geol. Karte der Schweiz, NF, XLIV. Lief.

STRECKEISEN, A. (1928): Geologie und Petrographie der Flüelagruppe. Schweiz. Mineral. Petrogr. Mitt., 8, 87-239..

THIERRIN, J. (1982): Géologie et pétrographie du Val Sarsura, Grison. Diploma, Universität Fribourg (unpublished).

THIERRIN, J. (1983): Les éclogites et le complexe gabbroique du val Sarsura (Silvretta). Schweiz. Mineral. Petrogr. Mitt., 63, 479-496.

THÖNI, M. (1981): Degree and evolution of the Alpine metamorphism in the Austroalpine Unit W of the Hohe Tauern in the light of K/Ar and Rb/Sr age determinations on micas. Jahrb. Geol. Bundesanst. (Austria), 124, 1, 111-174.

THÖNI, M. (1982): Der Einfluss der kretazischen Metamorphose im Westabschnitt der ostalpinen Einheit: Interpretation geochronologischer Daten. Mitt. Ges. Geol. Bergbaustud. Österr., 28, 17-34.

THÖNI, M. (1983): The termal climax of the early alpine metamorphism in the asutroalpine thrust sheet. Mem. Scienze geol. Padova, 36, 211-238.

THÖNI, M. (1988): personal communication.

TRACY, R. J. (1982): Compositional zoning and inclusions in metamorphic minerals. In: FERRY, J. M. (ed.): Characterization of metamorphism through mineral equilibria. Reviews in Mineralogy 10, Min. Soc. of America, 355-397.

WENK, E. (1934): Beiträge zur Petrographie und Geologie des Silvrettakristallins. Schweiz. Mineral. Petrogr. Mitt., 14, 196-278.

Manuscript received June 1, 1988; revised manuscript accepted September 15, 1988.